Automatic Analysis of Activation Recovery Interval in Heterogeneous Fibrotic Tissue from Chronically Infarcted Swine

Rafael Silva[1], Jairo Rodríguez-Padilla[1], Mihaela Pop[1, 2], Maxime Sermesant[1]

[1]Epione Research Team, Inria, Université Côte d'Azur, France
[2]Sunnybroook Research Institute Toronto, Canada

Abstract

Scar-related myocardial tissue can lead to ventricular arrhythmia (VA), a global concern for sudden cardiac death. Repolarization dispersion due to electrical remodeling within infarcted territory often triggers ventricular arrhythmias. However, evaluating ventricular repolarization globally is clinically challenging and there is no gold-standard approach. This paper introduces a new method using body-surface leads to automate activation (ATs) and recovery times (RTs) detection in unipolar electrograms (UEs). Multilevel Discrete Wavelet Transform sets activation and recovery detection windows based on external lead data. Then, Wyatt's method is used to compute ATs and RTs. By analyzing catheter-based intracardiac electrograms from n=9 infarcted swine, we compare ARI values between healthy tissue and arrhythmia-prone border zones (BZ), and between normal sinus rhythm (NSR) and pacing. Results reveal significant ARI differences between NSR and pacing, and among tissue types, with heterogeneous ARI values highlighting the repolarization complexity within BZ. This emphasizes the necessity for new automated approaches in assessing and treating cardiac arrhythmias, acknowledging the diverse electrophysiological individual profiles.

1. Introduction

Scar-related ventricular arrhythmia (VA) is a major cause of cardiac sudden cardiac death in the world. Electrical remodeling within and around scars causes a dispersion of repolarization, which is arrhythmogenic [1]; however, the global pattern of repolarization is difficult to assess clinically. Studies have shown the relationship between inhomogeneity of ventricular repolarization and enhanced ventricular arrhythmia vulnerability [2]. Refractory period, transmembrane action potential duration (APD), and activation recovery interval (ARI) are typically used to understand the properties of ventricular repolarization. ARI has the advantage of being able to be extracted from multiple recorded intracardiac electrograms (iEGMs) and is well-validated [3]. ARI can be obtained in vivo during invasive electrophysiological studies from pacing leads, allowing us to record unipolar electrogram signals (UE), and to approximate the depolarization and repolarization times via markers. The time corresponding to the steepest negative slope during the activation in the UE is widely accepted [4] as the depolarization time. Repolarization time is typically identified using the Wyatt method [5] as the steepest positive slope during the T wave; however, this definition is somewhat controversial. The ARI is defined as the time between activation time (AT) and repolarization time (RT) according to these markers and is often considered a clinical surrogate of action potential duration (APD). Thus, a better understanding of post-infarction ARI distribution could contribute towards an improved management of scar-related arrhythmias.

Our broad aim is to gain insight and add new knowledge to the impact the repolarization phase in healthy myocardial tissue and arrhythmogenic substrate might have on cardiac electrophysiological function. The substrate of scar-related ventricular arrhythmia consists of surviving bundles having altered electrical properties and is harbored at the border zone (BZ) located between healthy tissue and dense scars (i.e., fibrotic collagen). Specifically, in this study we sought to investigate the variability of the ARI distribution in heterogeneous fibrotic tissue, using UEs recorded in: (i) normal sinus rhythm (NSR); and, (ii) pacing conditions, from chronically infarcted swine. The endocardial iEGMs were recorded via intracardiac catheters maneuvered in the ventricular cavity (see detailed description in Data Source). For each of these two scenarios, we performed a comprehensive analysis on the whole cohort of cases, as well as per individual case. Figure 1 shows an example of a reconstructed map of local activation times, LAT (A) along with a bipolar voltage map (B) that is usually used to stratify the kind of tissue (healthy and BZ), as well as exemplary iEGMs (C) - (F) for the two different scenarios and tissue types (healthy and BZ).

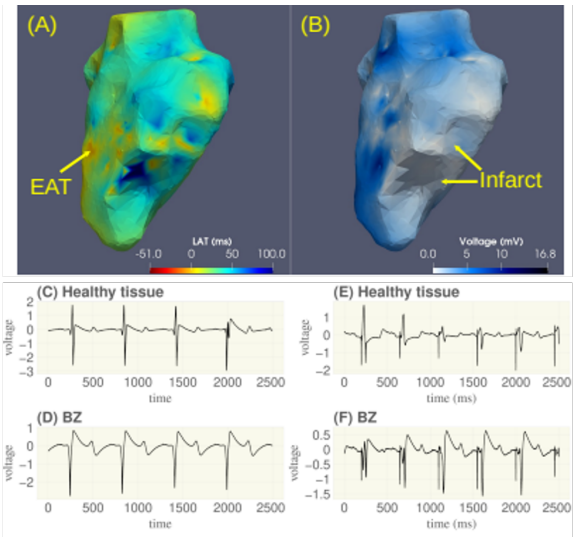

Figure 1. (A) Exemplary LAT map and (B) bipolar voltage map, recorded from a case during pacing. Frames (C) and (D) show an example of an iEGM for healthy and border zone, respectively, during sinus rhythm; Frames (E) and (F) show iEGM signals for pacing recordings.

Given the diverse morphological characteristics of EGM signals, here we propose to investigate the systematic use of an ECG lead to guide the automatic detection of ATs and RTs in UEs. Explicitly, using multilevel Discrete Wavelet Transform (DWT), we define activation and recovery detection windows based on information extracted from the external lead. The local ATs and RTs are computed according to Wyatt's method in these windows, and then ARI values are extracted. By doing so, we aim to improve accuracy and consistency in EGM interpretation and analysis. We also test our approach on real iEGM data and perform statistical analysis by stratifying the ARIs by heart rhythm type (NSR and pacing) and tissue (healthy and BZ).

2. Methodology and Proposed Approach

In this work, we propose a novel algorithm to automatically extract ATs and RTs from iEGM recordings and rapidly compute ARIs. Since there is no gold-standard approach, the proposed methodology is built on well-established signal processing techniques typically used to analyze ECG recordings with parameters tuned to specifically process EGM signals, which were empirically determined.

2.1. Signal Preprocessing and Fiducial Extraction

In order to avoid high-frequency components that could interfere with the subsequent signal analysis such as the derivative computation (sensitive to high-frequency noise), all EGM and ECG channels are first filtered using a low-pass Finite Impulse Response (FIR) filter with a 100 Hz cutoff frequency. Then, using the wavelet-based method of Martinez et. al [6], the P-wave onsets, T-wave offsets, and R-peak locations are extracted from the lead II channel of the body-surface ECG, which will serve as a reference lead when locating activation and recovery times. The derivative of the UE is computed with the first-order discrete differences, ensuring computational efficiency and preserving temporal accuracy of corresponding ATs and RTs of highly sampled recordings.

2.2. Detection of Activation and Recovery Times in Unipolar Electrograms

A novel customized algorithm was developed to detect ATs in UEs, assuming a 1 kHz sampling frequency. The *Symlet-4 wavele*t is first used to identify high-frequency components. Using a 9-level decomposition, detail coefficients 3 through 5 (corresponding to the 15,6 – 125 Hz frequency band) are used to create a signal version where peaks can easily be extracted. Then, using 100 ms windows centered around the peaks, the derivative minima are extracted, thus corresponding to the ATs as per Wyatt's method. Only ATs that coincide with R-peaks from lead II are selected (with a 50 ms tolerance). To pinpoint the recovery events in NSR, a recovery detection window is defined starting at 60 ms after the activation and, based on the available fiducials from lead II, up until: 20 ms after the lead II T-wave offset, if detected; at the lead II P-wave onset, if no T-wave offset was detected; or 20% before the next event, if no waves were detected on lead II. The same approach is used in pacing records; however, the recovery detection window is narrowed down to the time between T-wave onset and offset of lead II.

2.3. Stratifying Activation Recovery Intervals by Heart Rhythm and Tissue Type

To investigate the differences between ARI values for different heart rhythms (NSR vs paced) and tissue types (healthy and BZ), we propose to analyze the ARI distributions at the acquisition level, meaning that the ARI values for each UE channel are computed and averaged. Then, the data is aggregated by the channels corresponding to a specific tissue type, or by the heart rhythm during the acquisition. More precisely, the average peak-to-peak amplitude of bipolar EGMs is used to analyze ARI differences between healthy and border zone tissues. Following the findings of previous studies [7], we use the following amplitude intervals >1.5 mV and 0.5-1.5 mV to separate healthy tissue from BZ, respectively. The Mann–Whitney U two-sided test is employed to compare the distributions of ARI values for the variables under study,

both at the intra-subject and population levels. By assessing the statistical difference in distribution medians, this analysis should offer insights into the heterogeneity of ARIs.

3. Results and Discussion

3.1. Data Source

This work is specifically focused on a comprehensive retrospective analysis of iEGMs recorded from the left ventricular endocardium in 9 swine during X-ray-guided electrophysiological studies. Briefly, the catheter-based EP studies were performed at ~5 weeks post-infarction, in accordance with local ethical approval (Sunnybrook Research Institute, Toronto, CA), as per the methodology described in similar procedures [8]. By the end of this healing period, heterogeneous fibrosis had developed and matured within the infarcted region, and was comprised of dense scars and surviving BZ, which may form reentry circuits that sustain dangerous VA. An electro-anatomical CARTO3 mapping system (Biosense) was used to acquire the iEGM signals using a 1 kHz sampling rate, via a Pentaray NAV ECO catheter (J&J MedTech) introduced in the cavity of the left ventricle, LV. High-density endocardial maps of LV (~2900 iEGMs on average per all pigs) were recorded in sinus rhythm and pacing conditions (typically paced from right ventricle).

3.2. Algorithm Implementation

As previously described, the automatic detection of ATs and RTs involves using different signal processing techniques. To do so, we used open-source Python libraries to implement our methodology. More precisely, the fiducials from lead II were extracted using the Martinez et. al [6] implementation; the first-order differences of the UEs were computed using NumPy's `diff` function; and finally, Multilevel DWT was performed using the PyWavelets library, and peak detection on the reconstructed signal was made using the find_peaks function of SciPy's signal module. Figure 2 summarizes the results of the proposed method for pacing. After locating an "activation event" (green dashed line) as a high-frequency peak in the UE, the derivative minima are computed (green circles) around the peaks (green region), thus corresponding to the ATs. As expected, these activation events do not necessarily match the ATs, but they allowed us to define where the ATs should be found based on Wyatt's criterion as well as the recovery detection windows as informed by lead II. Notably, the detection windows are limited by the T-wave offsets identified in lead II.

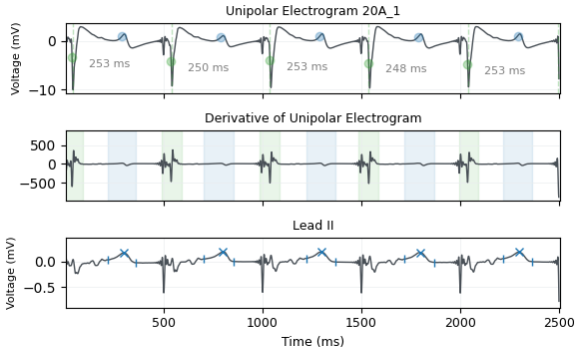

Figure 2. Analysis of an exemplary UE in pacing rhythm. **Top**: UE signal showing activation (green) and recovery (blue) times, and the corresponding ARIs. The dashed vertical lines correspond to an "activation event". **Middle**: first derivative of the UE signal, along with the detection windows for activation (green) and recovery (blue) times, used to find the minimum and maximum derivatives. **Bottom**: lead II and the detected fiducials, namely the R-peaks and T-wave limits.

3.3. Activation Recovery Interval Analysis

To showcase the relevance of our methodology, we present below the statistical analysis on the two types of data stratification using the extracted ARI values from the 9 acquired datasets. Figure 3 depicts the overall distribution of ARI values across all cases, in NSR and pacing conditions. The two distributions reveal significant disparities in mean ARI, suggesting differences in repolarization time in these heart rhythms. Also, the results from the Mann-Whitney U test at the individual level demonstrate significant differences between the distributions, with p-values below 1e-4.

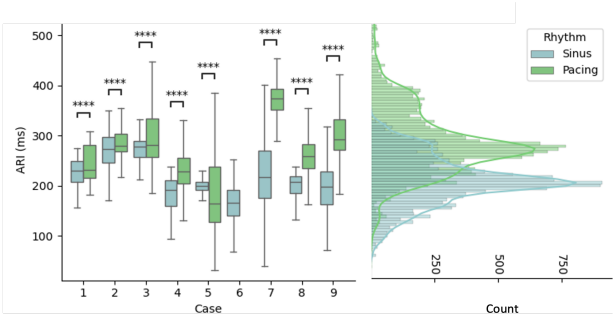

Figure 3. Distribution of rhythm-stratified ARI values per case (left) and the combined distribution (right). **** indicates p-value < 1e-4. Boxplots show quartiles and median values.

Figure 4 shows the ARI values separated based on the bipolar amplitudes in healthy and BZ tissues. In this case,

the combined distributions appear similar, with no statistically significant differences. However, at the case level, we observe heterogeneous results. For cases # 1, 2, 3, 8, and 9 the ARI values differ between healthy and BZ tissues, whereas for cases # 4, 5, 6, and 7 there are no distinguishable differences.

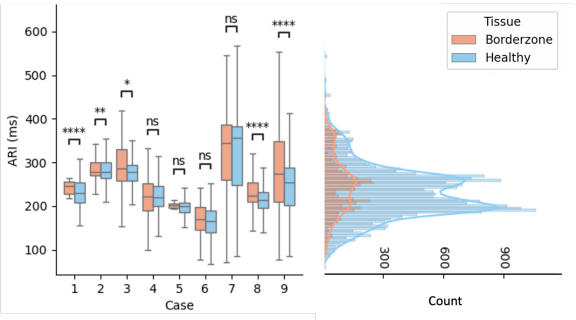

Figure 4. Distribution of tissue-stratified ARI values per case (left) and the combined distribution (right). Statistical significance: **** p-value < 1e-4, ** p-value < 1e-2, * p-value < 0.05, and 'ns' indicates not significant.

4. Conclusion

Our proposed method facilitates the systematic computation of activation recovery intervals in unipolar electrograms by integrating activation events detected in the signal with fiducial information from a body-surface lead. We use a multi-level DWT to define detection windows and identify activation times automatically. By using body-surface lead fiducials, such as T-wave, we determine recovery times. The significant differences observed in median ARIs between pacing and NSR rhythms highlight the importance of considering the heart rate in electrophysiological dynamics. Since the BZ located at the interface between healthy myocardium and dense scar harbors potentially arrhythmogenic substrates, studying the electrophysiological properties of tissue types is highly relevant for iEGM interpretation, as well as for accurate modeling of wave propagation and arrhythmia. With this respect, our heterogeneous ARI results at the case level emphasize the complexity of repolarization patterns within healthy and BZ tissues. These findings support the need for tailored approaches in both clinical assessment and interventions for cardiac arrhythmias, considering the diverse electrophysiological profiles across patients and tissue types.

Acknowledgments

This work was supported by the SimCardioTest project which has received funding from the European Union's Horizon 2020 research and innovation program under grant agreement No. 101016496, by the French government, through the 3IA Côte d'Azur Investments in the Future project managed by the National Research Agency (ANR) with the reference number ANR-19-P3IA-0002 and by Canadian CIHR project grant (PJT) 1532121, which also provided the preclinical data.

References

[1] J. Han and G. K. Moe, "Nonuniform recovery of excitability in ventricular muscle," Circ Res, vol. 14, pp. 44–60, 1964.
[2] J. Han, D. Millet, B. Chizzonitti, and G. K. Moe, "Temporal dispersion of recovery of excitability in atrium and ventricle as a function of heart rate," Am Heart J, vol. 71, pp. 481–487, 1966. PMID: 4951481.
[3] M. Potse, A. Vinet, T. Opthof, and R. Coronel, "Validation of a simple model for the morphology of the T wave in unipolar electrograms," Am J Physiol Heart Circ Physiol, vol. 297, pp. H792–H801, 2009.
[4] A. M. Yue, J. R. Paisey, S. Robinson, T. R. Betts, P. R. Roberts, and J. M. Morgan, "Determination of human ventricular repolarization by noncontact mapping: Validation with monophasic action potential recordings," Circulation, vol. 110, no. 11, pp. 1343–1350, 2004.
[5] R. Wyatt, M. Burgess, A. Evans, R. Lux, J. Abildskov, and T. Tsutsumi, "Estimation of ventricular trans-membrane action potential durations and repolarization times from unipolar electrograms," American Journal of Cardiology, vol. 47, p. 488, 1981.
[6] J. P. Martínez, R. Almeida, S. Olmos, A. P. Rocha, and P. Laguna, "A wavelet-based ECG delineator: evaluation on standard databases," IEEE Trans Biomed Eng, vol. 51, no. 4, pp. 570-581, Apr. 2004. doi: 10.1109/TBME.2003.821031. PMID: 15072211.
[7] M. Josephson and E. Anter, "Substrate Mapping for VT: Assumptions and Misconceptions," J Am Coll Cardiol EP, vol. 1, no. 5, pp. 341–352, Oct. 2015. https://doi.org/10.1016/j.jacep.2015.09.001.
[8] T. Escartin et al., "The extent of LGE-defined fibrosis predicts ventricular arrhythmia severity: insights from a preclinical model of chronic infarction," Lecture Notes in Computer Science, vol. 13958, pp. 698-707, 2023.

Address for correspondence:
Rafael Silva
Centre INRIA d'Université Côte d'Azur, EPIONE team
06902 Sophia Antipolis, France
rafael.silva@inria.fr